Dalton Transactions

COMMUNICATION

View Article Online
View Journal | View Issue



Cite this: *Dalton Trans.*, 2016, **45**, 11939

Received 24th April 2016,
Accepted 30th June 2016

DOI: 10.1039/c6dt01590e

www.rsc.org/dalton

# Ferrocene–quinoxaline Y-shaped chromophores as fascinating second-order NLO building blocks for long lasting highly active SHG polymeric films†

Kabali Senthilkumar,[a] Krishnan Thirumoorthy,[a] Claudia Dragonetti,[b,c] Daniele Marinotto,[b] Stefania Righetto,[b] Alessia Colombo,*[b] Matti Haukka[d] and Nallasamy Palanisami*[a]

**The first example of a Y-shaped ferrocene quinoxaline derivative with a surprisingly high and stable second harmonic generation (SHG) response in composite polymeric films is reported. The interesting quadratic hyperpolarizability values of different substituted Y-shaped chromophores are also investigated in solution by the EFISH technique.**

Materials with second-order nonlinear optical (NLO) properties are of great interest since they can be used for various important applications such as optical communication, optical data processing and storage, and electro-optical devices.[1]

Organic chromophores with particular shapes (H,[2] V,[3] Y,[4] X,[5] T[6] and star[7] type) are interesting for electro-optic applications and their arrangement ensures efficient intramolecular charge transfer (ICT) between the donor and acceptor moieties and generates the push–pull system featuring low-energy and intense CT absorption.[8] Due to the ICT, the push–pull donor–π-acceptor (D–π-A) molecules possess distinct nonlinear optical (NLO) properties.

Coordination compounds are a growing class of second-order NLO chromophores that can offer additional flexibility, when compared to organic compounds, due to the presence of metal–ligand charge-transfer between the metal and the ligands usually of high intensity and at relatively low energy, tunable by nature, oxidation state and coordination sphere of the metal center.[9]

Heteroaromatic moieties incorporated into an NLO chromophore may act as auxiliary D or A and further improve the optical nonlinearity of the chromophore. Quinoxalines/pyrazines have been widely used in chromophore systems as a strong electron acceptor because of their high electron deficiency originating from the two symmetric unsaturated nitrogen atoms that lower the π* level of the conjugated system.[10] Limited information on the Y-shaped chromophores based on a quinoxaline moiety for NLO and dye-sensitized solar cells (DSSCs) is available in the literature.[11] In particular Bureš *et al.*, studied the structure–property relationship and NLO properties for different substituted pyrazine push–pull chromophores with various π-linkers.[5b,6,11b]

In the field of NLO, ferrocene derivatives have been deeply investigated and have played the role of an electron-donor in charge transfer processes in chromophores where ferrocene is linked to an acceptor moiety.[9b,12]

Although ferrocene–quinoxaline based Y-shaped chromophores, recently reported by Kumar *et al.*, show interesting DSSC performance,[13] their NLO properties have never been investigated. This type of organometallic based Y-shaped chromophore structure allows good coupling between the d orbitals of the metal and π* system of the quinoxaline moiety that could afford a significant NLO response controlled by low-energy metal ligand charge transfer (MLCT) transitions.

Keeping this in mind, we have synthesized Y-shaped chromophores by condensation of a 1,6-bis-ferrocenyl-hexa-1,5-diene-3,4-dione with a substituted 1,2-diamino compound; this is one of the most versatile methods and was used for the construction of quinoxaline derivatives, **YQ1**, **YQ2**, **YQ5**, and **YQ6**; for **YQ3** and **YQ4**, a different synthetic strategy was used as shown in Scheme S1.†

The Y-shaped substituted quinoxaline derivatives **YQ1–YQ6** were characterized by using FT-IR, $^1$H-NMR, and mass and single crystal X-ray diffraction techniques (ESI†). The single crystal X-ray structure of **YQ1** and **YQ2** (Fig. 1) shows a Y-shaped structure and the ferrocene moieties are facing the antennae type. The structural parameters obtained from X-ray

[a]*Department of Chemistry, School of Advanced Sciences, VIT University, Vellore 632014, Tamilnadu, India. E-mail: palanisami.n@gmail.com; Tel: +91 98426 39776*
[b]*Department of Chemistry and Centro CIMAINA, University of Milan, INSTM-Research Unit, Via C. Golgi 19, 20133 Milan, Italy. E-mail: alessia.colombo@unimi.it*
[c]*ISTM-CNR via Golgi 19 Milan, Italy*
[d]*Department of Chemistry, University of Jyväskylä, P.O. Box 35, FI-40014 Jyväskylä, Finland*

†Electronic supplementary information (ESI) available: X-ray crystallographic data, theoretical details, cartesian coordinates, and all experimental details. CCDC 1440374 and 1440375. For ESI and crystallographic data in CIF or other electronic format see DOI: 10.1039/c6dt01590e

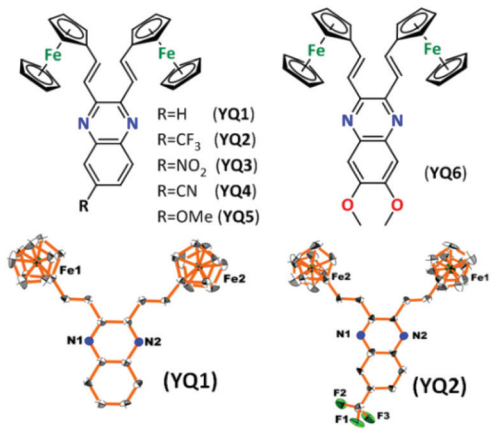


Fig. 1 Chemical structures of Y-shaped ferrocene-based chromophores **YQ1–YQ6** and single crystal X-ray structures of chromophores **YQ1** and **YQ2** (30% probability ellipsoids). Hydrogen atoms are omitted for clarity.

analysis closely matches with the optimized structures obtained from density functional theory (DFT) studies at B3LYP/6-31+G** level of theory (ESI†) except that there is a slight difference in the values of the dihedral angles with respect to the substituents (H and $CF_3$). This may be due to the solid state packing and the associated intermolecular hydrogen bonding (ESI†).

The absorption spectra in $CH_2Cl_2$ of chromophores **YQ1–YQ6** show variably intense CT absorption bands as reported in Fig. 2. All molecules depict prominent absorption bands in the

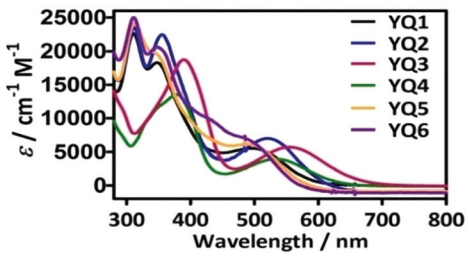


Fig. 2 Absorption spectra of **YQ1–YQ6** in $CH_2Cl_2$ at 298 K.

UV region which can safely be ascribed to a high energy ligand-centred π–π* electronic transition (ICT transition). The other bands in the visible region can be assigned to other localized excitations with a lower energy produced either by two nearly degenerate transitions, a Fe(II) d–d transition (assigned to $^1E_{1g} \leftarrow {}^1A_{1g}$) or by an MLCT process (dπ–π*).[14] By increasing the strength of R as an electron withdrawing group on the quinoxaline scaffold, a bathochromic shift is observed. The detailed absorption bands and their energy gap are given in Table 1.

To gain insight into the structural and electronic properties of chromophores **YQ1–YQ6**, we performed DFT and time-dependent DFT (TD-DFT) calculations using Gaussian 09 software.[15] The main optimized geometrical parameters and calculated highest occupied molecular orbital (HOMO) and lowest unoccupied molecular orbital (LUMO) energies, absorption maxima ($\lambda_{max}$), are reported in Table 1 (ESI†). The lowest energy electronic transitions for all the quinoxaline chromophores originate from the HOMO to LUMO. The HOMO–LUMO energy gap decreases by increasing the strength of the acceptor, and the experimental results confirm this trend as evidenced by a red shift of the MLCT band. The density plots of HOMO and LUMO levels and their energy gaps are influenced by the electron donor, ferrocene, π-spacer and acceptor quinoxaline derivative strength. The HOMO is mainly localized on the ferrocene moiety and π-spacer double bond, whereas the electron density in the LUMO is mainly localized on the substituted quinoxaline moiety (Fig. 3). The HOMO energies of chromophores **YQ1–YQ6** are quite similar (−5.6 to −5.3 eV) while their LUMO energies are influenced by virtue of the nature of R substituents. The biggest destabilizations are observed when R is an electron-donor substituent (**YQ5** and **YQ6**) reaching values ranging from −2.80 to 2.24 eV. Therefore, the increased HOMO–LUMO gap calculated for all the chromophores is essentially related to LUMO destabilization. The calculated absorption maxima of the chromophores originate by single HOMO–LUMO transitions (at 3.12 to 2.64 eV/397 to 469 nm) based on the DFT calculations. The theoretically observed trend is comparable with the experimental values. The absolute values vary by the range of 100 nm with experimental values which are due to the limitation in the basis set used for calculations. The calculated data and main transitions

Table 1 Photophysical data and second order NLO properties of the investigated chromophores **YQ1–YQ6**

| Sample | $\lambda_{max}^{HE}$ [nm (eV)]/$\varepsilon^a$ (×10$^3$) [M$^{-1}$ cm$^{-1}$] | $\lambda_{max}^{LE}$ [nm (eV)]/$\varepsilon^a$ (×10$^3$) [M$^{-1}$ cm$^{-1}$] | HOMO$^b$ (eV) | LUMO$^b$ (eV) | $\lambda_{max}{}^b$ [nm (eV)] | $\mu^{b,d}$ (×10$^{-18}$ esu) | $\mu\beta^e$ (×10$^{-48}$ esu) |
|---|---|---|---|---|---|---|---|
| **YQ1** | 349 (3.55)/17.5 | 498 (2.48)/0.55 | −5.40 | −2.29 | 397 (3.12) | 3.4 | −790 |
| **YQ2** | 356 (3.48)/22.1 | 522 (2.37)/0.68 | −5.37 | −2.37 | 413 (2.99) | 5.9 | −960 |
| **YQ3** | 389 (3.18)/18.7 | 558 (2.22)/0.57 | −5.45 | −2.80 | 469 (2.64) | 6.3 | −820 |
| **YQ4** | 379 (3.27)/12.8 | 536 (2.31)/0.39 | −5.63 | −2.74 | 430 (2.88) | 5.5 | −560 |
| **YQ5** | 350 (3.54)/20.1 | 501 (2.47)/0.61 | −5.37 | −2.25 | 397 (3.11) | 1.1 | −580 |
| **YQ6** | 352 (3.52)/19.8 | 499 (2.48)/0.64$^c$ | −5.35 | −2.24 | 398 (3.11) | 1.3 | −430 |

$^a$ Experimental data (HE = high energy, LE = low energy). $^b$ Theoretical data calculated with B3LYP/6-31+G** theory. $^c$ Shoulder. $^d$ For compounds **YQ2**, **YQ3** and **YQ4**, the values were also determined experimentally in $CHCl_3$ (3.3, 3.4 and 2.1 × 10$^{-18}$ esu, respectively). $^e$ In anhydrous $CHCl_3$ estimated uncertainty in EFISH measurements ± 10%.

 

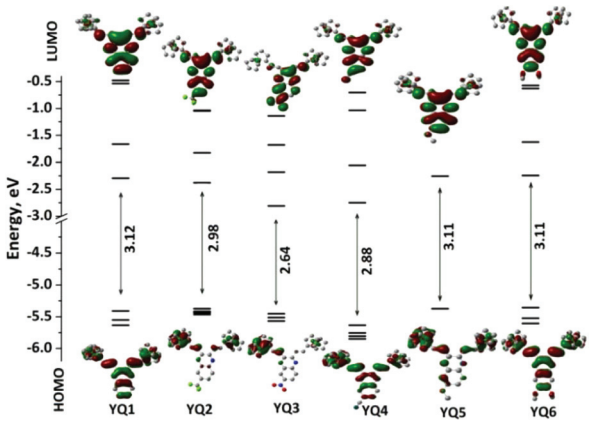


**Fig. 3** Schematic representation of the energy levels of chromophores **YQ1–YQ6** at B3LYP/6-31+G** level of theory. Isodensity surface plots of HOMO and LUMO molecular orbitals are also shown.

involved in the principle orbitals are given as density plots in the ESI.†

Here we report the second-order NLO properties in $CHCl_3$ solution of all the chromophores, using the electric field induced second harmonic (EFISH) generation technique.[16] This technique offers a valuable alternative to Hyper-Rayleigh scattering (HRS) which suffers from the limitation of possible overestimation of values of the quadratic hyperpolarizability due to multiphoton fluorescence. EFISH can provide direct information on the intrinsic molecular NLO properties through eqn (1):

$$\gamma_{\mathrm{EFISH}} = (\mu\beta_{\lambda}/5kT) + \gamma(-2\omega;\omega,\omega,0) \quad (1)$$

where $\mu\beta_{\mathrm{EFISH}}/5kT$ is the dipolar orientational contribution to the molecular nonlinearity, and $\gamma(-2\omega, \omega, \omega, 0)$, the third order polarizability at frequency $\omega$ of the incident light, is a purely electronic cubic contribution to $\gamma_{\mathrm{EFISH}}$ which can usually be neglected when studying the second-order NLO properties of dipolar compounds. Chromophores **YQ1–YQ6** are characterized by good to excellent values of $\mu\beta_{\mathrm{EFISH}}$ ($-430$ to $-960 \times 10^{-48}$ esu), see Table 1, working in $CHCl_3$ at a concentration of $10^{-3}$ M with a non-resonant incident wavelength of 1.907 μm, obtained by Raman-shifting under high $H_2$ pressure by using a Q-switched, mode-locked $Nd^{3+}$:YAG laser. The largest $\mu\beta_{\mathrm{EFISH}}$ values are observed for $CF_3$ (**YQ2**) and $NO_2$ (**YQ3**) derivatives. In order to obtain the projection along the dipole moment axis of a vectorial component of the tensor of the quadratic hyperpolarizability ($\beta_{\mathrm{EFISH}}$), it is necessary to know the dipole moment, $\mu$. So in this work, we have calculated the theoretical dipole moments (B3LYP/6-31+G**) of all the chromophores. For comparison, we have also experimentally determined the dipole moments in $CHCl_3$ for compounds **YQ2**, **YQ3**, and **YQ4** (Table 1) using the Guggenheim's method.[17] Experimental values follow the same trend of theoretical ones but are lower than the calculated dipole moments, in accordance with the literature.[18]

The investigated chromophores show a "push–pull" Y-shaped structure which is the origin of a non- zero dipole moment and it is directed from the symmetrical ferrocenyl moiety as a positive pole to quinoxaline moiety as a negative pole (ESI†).

The substituents are responsible for the different ground state dipole moments: on going from **YQ1** (R = H) to **YQ2–YQ4** (R = electron withdrawing group) there is an increase of the dipole moment, whereas on going from **YQ1** (R = H) to **YQ5–YQ6** (R = electron donor group) a decrease of the dipole moment occurs (Table 1). These data show that the origin of the high $\mu\beta$ values of **YQ2** and **YQ3** is a particularly high dipole moment. Surprisingly, although second order NLO properties both in solution and in the solid-state of many ferrocene derivatives have been investigated,[9b] only a few works of thin films of pure ferrocene or ferrocene derivatives have been published.[19] Host–guest polymethylmethacrylate (PMMA) films with ferrocene were reported[20] but the films were studied for their luminescence properties only. To our knowledge, no SHG measurements of PMMA films with ferrocene guests have been reported. When dipolar chromophores are introduced into polymeric systems as dopants, a highly polar push–pull structure usually leads to centrosymmetric alignment, due to the strong electronic interactions. However, only those materials lacking centrosymmetry could exhibit nonzero macroscopic second-order susceptibility. A convenient method to achieve the non-centrosymmetric alignment of chromophore moieties with high $\mu$ is to heat the film to a temperature near the glass transition temperature of the polymer ($T_g$) in the presence of an electric field, leading to the poling-induced non-centrosymmetric alignment of chromophores.[21]

The high quadratic hyperpolarizability value of chromophore **YQ2** in solution prompted us to investigate its potential as a molecular building block for composite films with SHG properties. It was dispersed both in PMMA and polystyrene (PS) matrices (5 wt% of chromophore with respect to the matrix) and oriented by poling (ESI†). The corona wire poling dynamics of the SHG behavior of polystyrene and the PMMA composite film are reported in Fig. 4. The UV-Vis absorption spectra after and before poling and the SEM images of **YQ2** in polystyrene and in PMMA films are reported in Fig. S1 and S3,† respectively. The second order NLO coefficient $d_{33}$ for poled films was obtained by following the standard Maker fringe technique (see the ESI†).

We found excellent $d_{33}$ values both in PS and in PMMA ($d_{33}$ values of 2.96 pm $V^{-1}$ and 5.27 pm $V^{-1}$, respectively. For $d_{33}$ calculation, see the ESI†); remarkably to our knowledge, the $d_{33}$ value in PMMA is the highest ever reported for a host/guest system based on organometallic chromophores. Surprisingly, the SHG signal remains unchanged also when the electric field is switched off. Its stability is remarkable, after four months, we found a $d_{33}$ value of 1.72 pm $V^{-1}$, with a stability of 33%. It is worth pointing out that the PMMA system gives an SHG response higher than polystyrene, but a higher stability (50%) is achieved using polystyrene as a matrix ($d_{33}$ of 1.47 pm $V^{-1}$).

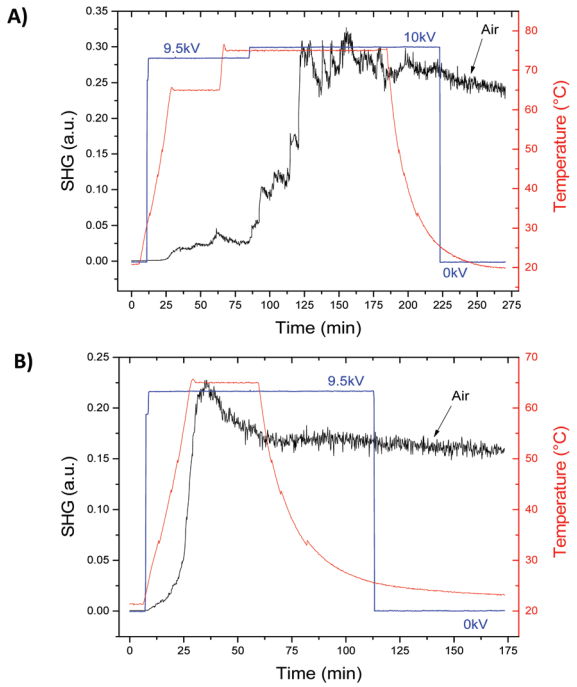


**Fig. 4** *In situ* corona-wire poling dynamics for chromophore **YQ2** in polystyrene (A) and in PMMA (B) thin films. The film thicknesses are 1.85 μm and 0.85 μm, respectively.

In conclusion, the reported Y-shaped chromophores containing ferrocene and a quinoxaline core have good second order nonlinear optical properties in solution and the really high $d_{33}$ value of the host/guest film in PMMA of **YQ2** makes those chromophores fascinating building blocks to obtain long lasting NLO-active polymeric films.

KSK thanks DST for the Inspire fellowship (IF-110138). KSK and NP gratefully acknowledge SIF DST-VIT-FIST, VIT University, Vellore for providing NMR, and IR data, and CDRI-Lucknow and IIT-Madras for HR-mass spectral analysis. We thank Dr Daniela Meroni for the SEM images.

## Notes and references

1 (*a*) J. Zyss and D. S. Chemla, in *Nonlinear Optical Properties of Organic Molecules and Crystals*, Elsevier, 1987, pp. 23–191; (*b*) N. P. Prasad and D. J. Williams, in *Introduction to Nonlinear Optical Effects in molecules and Polymers*, Wiley, 1991; (*c*) J. Zyss, in *Molecular Nonlinear Optics: Materials, Physics and Devices*, Academic Press, Boston, 1994; (*d*) D. R. Kanis, M. A. Ratner and T. J. Marks, *Chem. Rev.*, 1994, **94**, 195–242; (*e*) S. R. Marder, *Chem. Commun.*, 2006, 131–134; (*f*) G. S. He, L.-S. Tan, Q. Zheng and P. N. Prasad, *Chem. Rev.*, 2008, **108**, 1245–1330; (*g*) J. Zyss, in *Molecular Nonlinear Optics: Materials, Physics, and Devices*, Academic Press, Boston, 2013.

2 W. Wu, C. Ye, J. Qin and Z. Li, *ChemPlusChem*, 2013, **78**, 1523–1529.

3 (*a*) F. Momicchioli, G. Ponterini and D. Vanossi, *Phys. Chem. Chem. Phys.*, 2014, **16**, 15576–15589; (*b*) R. Andreu, E. Galán, J. Garín, V. Herrero, E. Lacarra, J. Orduna, R. Alicante and B. Villacampa, *J. Org. Chem.*, 2010, **75**, 1684–1692.

4 M. Pokladko-Kowar, N. Nosidlak, E. Gondek, I. V. Kityk, F. Bureš, J. Kulhánek and P. Karasiński, *Opt. Quantum Electron.*, 2016, **48**, 82.

5 (*a*) H. Kang, G. Evmenenko, P. Dutta, K. Clays, K. Song and T. J. Marks, *J. Am. Chem. Soc.*, 2006, **128**, 6194–6205; (*b*) L. Dokládalová, F. Bureš, W. Kuznik, I. V. Kityk, A. Wojciechowski, T. Mikysek, N. Almonasy, M. Ramaiyan, Z. Padělková, J. Kulhánek and M. Ludwig, *Org. Biomol. Chem.*, 2014, **12**, 5517–5527.

6 P. Solanke, F. Bureš, O. Pytela, M. Klikar, T. Mikysek, L. Mager, A. Barsella and Z. Růžičková, *Eur. J. Org. Chem.*, 2015, 5339–5349.

7 W. Wu, C. Wang, C. Zhong, C. Ye, G. Qiu, J. Qin and Z. Li, *Polym. Chem.*, 2013, **4**, 378–386.

8 (*a*) S. Matsumoto, M. Akazome, S. Qu, T. Kobayashi, M. Kanehiro and K. Ogura, *Heterocycles*, 2010, **80**, 645; (*b*) W. Chen, T. Salim, H. Fan, L. James, Y. M. Lam and Q. Zhang, *RSC Adv.*, 2014, **4**, 25291; (*c*) C. Y. Jung, C. J. Song, W. Yao, J. M. Park, I. H. Hyun, D. H. Seong and J. Y. Jaung, *Dyes Pigm.*, 2015, **121**, 204–210; (*d*) K. Pei, Y. Wu, H. Li, Z. Geng, H. Tian and W.-H. Zhu, *ACS Appl. Mater. Interfaces*, 2015, **7**, 5296–5304.

9 (*a*) I. D. L. Albert, T. J. Marks and M. A. Ratner, *J. Am. Chem. Soc.*, 1997, **119**, 6575–6582; (*b*) S. Di Bella, C. Dragonetti, M. Pizzotti, D. Roberto, F. Tessore and R. Ugo, in *Topics in Organometallic Chemistry 28. Molecular Organometallic Materials for Optics*, ed. H. Le Bozec and V. Guerchais, Springer Verlag, Berlin Heidelberg, 2010, pp. 1–55; (*c*) A. Valore, M. Balordi, A. Colombo, C. Dragonetti, S. Righetto, D. Roberto, R. Ugo, T. Benincori, G. Rampinini, F. Sannicolò and F. Demartin, *Dalton Trans.*, 2010, **39**, 10314–10318; (*d*) E. Rossi, A. Colombo, C. Dragonetti, S. Righetto, D. Roberto, R. Ugo, A. Valore, J. A. G. Williams, M. G. Lobello, F. De Angelis, S. Fantacci, I. Ledoux-Rak, A. Singh and J. Zyss, *Chem. – Eur. J.*, 2013, **19**, 9875–9883.

10 (*a*) T. Yamamoto, T. Kanbara, N. Ooba and S. Tomaru, *Chem. Lett.*, 1994, 1709–1712; (*b*) C. Dragonetti, M. Pizzotti, D. Roberto and S. Galli, *Inorg. Chim. Acta*, 2002, **330**, 128–135; (*c*) M. Pizzotti, R. Ugo, D. Roberto, S. Bruni, P. Fantucci and C. Rovizzi, *Organometallics*, 2002, **21**, 5830–5840; (*d*) Y. Wu and W. Zhu, *Chem. Soc. Rev.*, 2013, **42**, 2039–2058.

11 (*a*) D. W. Chang, H. J. Lee, J. H. Kim, S. Y. Park, S. M. Park, L. Dai and J. B. Baek, *Org. Lett.*, 2011, **13**, 3880–3883; (*b*) F. Bureš, H. Čermáková, J. Kulhánek, M. Ludwig, W. Kuznik, I. V. Kityk, T. Mikysek and A. Růžička, *Eur. J. Org. Chem.*, 2012, 529–538; (*c*) K. Pei, Y. Wu, A. Islam, S. Zhu, L. Han, Z. Geng and W. Zhu, *J. Phys. Chem. C*, 2014, **118**, 16552–16561.

12 (*a*) S. Scuppa, L. Orian, D. Dini, S. Santi and M. Meneghetti, *J. Phys. Chem. A*, 2009, **113**, 9286–9294; (*b*) M. Zaarour, A. Singh, C. Latouche, J. A. G. Williams, I. Ledoux-Rak, J. Zyss, A. Boucekkine, H. Le Bozec, V. Guerchais, C. Dragonetti, A. Colombo, D. Roberto and A. Valore, *Inorg. Chem.*, 2013, **52**, 7987–7994.

13 R. Chauhan, M. Shahid, M. Trivedi, D. P. Amalnerkar and A. Kumar, *Eur. J. Inorg. Chem.*, 2015, 3700–3707.

14 (*a*) C. T. Sanderson, J. A. Quinlan, R. C. Conover, M. K. Johnson, M. Murphy, R. A. Dluhy and C. Kutal, *Inorg. Chem.*, 2005, **44**, 3283–3289; (*b*) S. Barlow, H. E. Bunting, C. Ringham, J. C. Green, G. U. Bublitz, S. G. Boxer, J. W. Perry and S. R. Marder, *J. Am. Chem. Soc.*, 1999, **121**, 3715–3723.

15 (*a*) M. J. Frisch, *et al.*, *Gaussian09 Rev. C.01*, Gaussian, Inc., Wallingford CT, 2009; (*b*) R. L. Martin, *J. Chem. Phys.*, 2003, **118**, 4775.

16 (*a*) B. F. Levine and C. G. Bethea, *J. Chem. Phys.*, 1975, **63**, 2666–2682; (*b*) I. Ledoux and J. Zyss, *J. Chem. Phys.*, 1982, **73**, 203–213.

17 E. A. Guggenheim, *Trans. Faraday Soc.*, 1949, **45**, 714–720.

18 V. Calabrese, S. Quici, E. Rossi, E. Criati, C. Dragonetti, D. Roberto, E. Tordin, F. De Angelis and F. Fantacci, *Chem. Commun.*, 2010, **46**, 8374–8376.

19 (*a*) A. Matei, C. Constantinescu, V. Ion, B. Mitu, I. Ionita, M. Dinescu, C. Vasiliu and A. Emandi, *J. Organomet. Chem.*, 2014, **751**, 638–643; (*b*) C. Constantinescu, A. Matei, V. Ion, B. Mitu, I. Ionita, M. Dinescu, C. R. Luculescu, C. Vasiliu and A. Emandi, *Appl. Surf. Sci.*, 2014, **302**, 83–86.

20 (*a*) D. Basak and B. Mallik, *Synth. Met.*, 2006, **156**, 176–184; (*b*) A. Thander and B. Mallik, *Solid State Commun.*, 1999, **111**, 341–346; (*c*) A. Thander and B. Mallik, *Chem. Phys. Lett.*, 2000, **330**, 521–527; (*d*) A. Thander and B. Mallik, *Solid State Commun.*, 2002, **121**, 159–164; (*e*) D. Basak and B. Mallik, *Synth. Met.*, 2004, **146**, 151–158.

21 (*a*) F. Nisic, A. Colombo, C. Dragonetti, M. Fontani, D. Marinotto, S. Righetto, D. Roberto and J. A. G. Williams, *J. Mater. Chem. C*, 2015, **3**, 7421–7427; (*b*) D. Marinotto, S. Proutière, C. Dragonetti, A. Colombo, P. Ferruti, D. Pedron, M. C. Ubaldi and S. Pietralunga, *J. Non-Cryst. Solids*, 2011, **357**, 2075–2080; (*c*) D. Marinotto, R. Castagna, S. Righetto, C. Dragonetti, A. Colombo, C. Bertarelli, M. Garbugli and G. Lanzani, *J. Phys. Chem. C*, 2011, **115**, 20425–20432; (*d*) A. Colombo, C. Dragonetti, D. Marinotto, S. Righetto, D. Roberto, S. Tavazzi, M. Escadeillas, V. Guerchais, H. Le Bozec, A. Boucekkine and C. Latouche, *Organometallics*, 2013, **32**, 3890–3894; (*e*) J. Boixel, V. Guerchais, H. Le Bozec, D. Jacquemin, A. Amar, A. Boucekkine, A. Colombo, C. Dragonetti, D. Marinotto, D. Roberto, S. Righetto and R. De Angelis, *J. Am. Chem. Soc.*, 2014, **136**, 5367–5375; (*f*) C. Dragonetti, A. Colombo, D. Marinotto, S. Righetto, D. Roberto, A. Valore, M. Escadeillas, V. Guerchais, H. Le Bozec, A. Boucekkine and C. Latouche, *J. Organomet. Chem.*, 2014, **751**, 568–572.